The Effect of the Production Process and Heat Processing Parameters on the Fatigue Strength of High-Grade Medium-Carbon Steel

T. Lipiński*, A. Wach

University of Warmia and Mazury in Olsztyn, The Faculty of Technical Sciences Department of Materials Technology,
St: Oczapowskiego 11, 10-957 Olsztyn, Poland
*Corresponding author. E-mail address: tomasz.lipinski@uwm.edu.pl

Abstract

The experimental material consisted of semi-finished products of high-grade, medium-carbon constructional steel with: manganese, chromium, nickel, molybdenum and boron. The experimental material consisted of steel products obtained in three metallurgical processes: electric and desulfurized (E), electric and desulfurized with argon-refined (EA) and oxygen converter with vacuum degassed of steel (KP). The production process involved two melting technologies: in a 140-ton basic arc furnace with desulphurisation and argon refining variants, and in a 100-ton oxygen converter. Billet samples were collected to analyze: relative volume of impurities, microstructure and fatigue tests. The samples were quenched and austenitized at a temperature of 880ºC for 30 minutes. They were then cooled in water and tempered by holding the sections at a temperature of 200, 300, 400, 500 and 600ºC for 120 minutes and air-cooled. Fatigue tests were performed with the use of a rotary bending machine at a frequency of 6000 cpm. The results were statistical processed and presented in graphic form. This paper discusses the results of microstructural analyses, the distribution of the relative volume of impurities in different size ranges, the fatigue strength characteristics of different production processes, the average number of sample-damaging cycles and the average values of the fatigue strength coefficient for various heat processing options.

Keywords: Heat Treatment, Metallography, Steel, Fatigue Strength, Fatigue Durability, Production Process

1. Introduction

Although steel has a relatively small number of non-metallic inclusions, those impurities have a considerable impact on the material's technological and strength parameters, in particular fatigue strength and life. The composition of technical iron alloys is inclusive of sulfur and oxygen. Those elements form solutions in liquid metal. Then the presence of oxygen and non-metallic inclusions in steel is a natural consequences of physical and chemical processes during production. The shape of non-metallic inclusions may vary. Spheroidal inclusions are characteristic of steel which contains high levels of oxygen. The addition of small amounts of aluminum leads to partial deoxydation of steel and the formation of inclusions along the boundaries of austenite grains. Excessive amounts of powerful deoxidants contribute to the formation of large faceted inclusions [1-8].

The distribution of inclusions is an equally important factor. Single inclusions and clusters of inclusions exert different effects. Large, individual inclusions can produce discontinuities that grow rapidly under variable load. The clusters of microparticles of

a subcritical size lower stress and increase the number of sample-damaging cycles [4, 9].

The effect of impurities is closely related to the processes taking place in micro-areas, which is why the size of inclusion particles significantly influences the properties of constructional materials.

During processing, the shape and distribution of microparticles change, and impurities undergo anisotropic deformation. Non-metallic inclusions play a special role in the process of steel hardening. Due to differences in the physical properties of steel and inclusion-forming phases, structural stresses are formed along inclusion boundaries. Fatigue cracking is caused by local discontinuities which are transformed into micro-cracks and cause material decohesion [10-12].

The combination of inner structural stresses caused by the presence of non-metallic inclusions and stresses resulting from external load plays an important role in the formation and development of fatigue cracks. Structural stresses are a function of inclusion structure. They are mostly affected by heat processing temperature when thermal stresses are formed along the inclusion-matrix (steel structure) boundary [3, 13-17]. The intensity and rate of micro-crack formation and stress levels that cause fatigue cracking are determined by the resistance encountered by migrating dislocations. Tensile strength and material hardness are measures of that resistance [18-19].

High-plasticity steel has been scantly researched in studies investigating the purity and fatigue life of steel subjected to variable load. Having regard to the general scarcity of relevant data, this study was undertaken to investigate the fatigue strength of high-plasticity steel, subject to stress, heat processing and production parameters.

2. Aim of the study and methods

The aim of this study was to determine the effect of the production process of high-grade medium-carbon steel, in particular out-of-furnace treatment and tempering temperature, on the distribution of the relative volume of impurities in various size ranges and fatigue strength parameters for different production processes, the average number of sample-damaging cycles and the average values of the fatigue strength coefficient for different heat processing options. The experimental material consisted of steel products obtained in three metallurgical processes: electric (E), electric with argon refining (EA) and oxygen conversion with wacuum (KP). The process of steel production was introduced in detail in [5, 20].

Analyses of fatigue stress with an oscillating cycle were carried out in accordance with Polish Standard PN-76/H-04326 using smooth steel samples with a fixed cross-section diameter of 10 mm. The applied analytical methodology was described by [3, 5].

The analyzed correlations between the tested parameters can take on form (1):

$$\sigma = a - b \cdot \log N \qquad (1)$$

or form (2) in an inverse function where the dependent variable is logN:

$$\log N = m - k \cdot \sigma \qquad (2)$$

where: m and p are material constants:
m- initial ordinate of curve,
k- angular coefficient of curve.

The least squares method was used to develop regression equations illustrating the correlation between the number of sample-damaging cycles within the endurance limit and the level of fatigue-inducing load. Student's t-test and the Fischer-Snedecor distribution test were used to compare statistical parameters and the correlations between the analyzed parameters.

To facilitate analyses of dependent variable logN, a diagram of function (2) was used, where the objective function is placed on the Y-axis and the independent variable – on the X-axis.

The level of fatigue-inducing load was adapted to the strength properties of steel. Maximum load was set at:
- for steel tempered at a temperature of 200°C - 650 MPa,
- for steel tempered at a temperature of 300°C - 500°C - 600 MPa,
- for steel tempered at a temperature of 600°C - 540 MPa.

During the test, the applied load was gradually reduced in steps of 40 MPa (to support the determinations within the endurance limit). Load values were selected to produce 10^4-10^6 cycles characterizing endurance limits [11]. Fatigue strength was measured, and its distribution was identified within the endurance limit, and the apparent fatigue strength limit was set.

3. The results of investigations and their analysis

The microstructure of specimens after various heat treatments is presented in Figures 1-5.
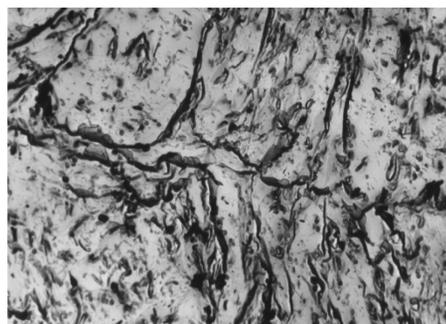
Fig. 1. Microstructure of steel involving an electric furnace desulfurized and argon refining (EA) and hardened and tempered at 200°C. Tempered martensite. Mag. 2000x
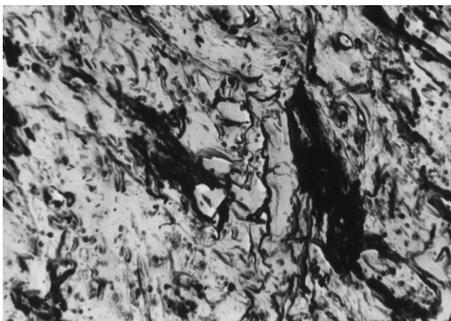
Fig. 2. Microstructure of steel involving an electric furnace desulfurized and argon refining (EA) and hardened and tempered at 300°C. Tempered martensite with metastable carbides. Mag. 2000x
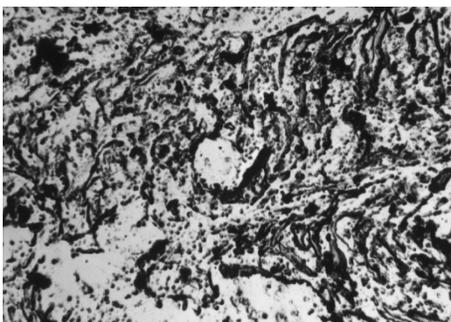
Fig. 3. Microstructure of steel involving an electric furnace desulfurized and argon refining (EA) and hardened and tempered at 400°C. Tempered martensite with cementite formations coherently bonded with the groundmass. Mag. 2000x
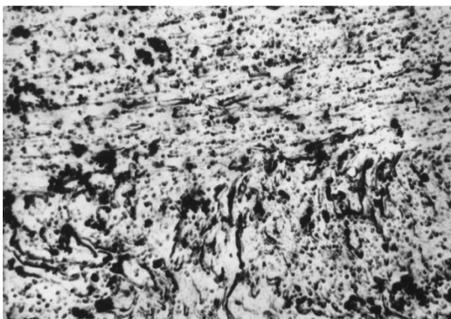
Fig. 4. Microstructure of steel involving an electric furnace desulfurized and argon refining (EA) and hardened and tempered at 500°C. Sorbit – mixture of ferryt and submicroscopic carbidies. Mag. 2000x

The observations of microstructures etched with nital revealed that steel hardening and tempering at various temperatures had different phase microstructure.

Variations in heat processing conditions produced the following structures during steel hardening: various forms of tempered tetragonal martensite structures (Fig. 1-3), sorbite and spheroidite (Fig. 5). Microstructure was determined solely by the

applied hardening technology (tempering temperature), and it was not affected by the production process.
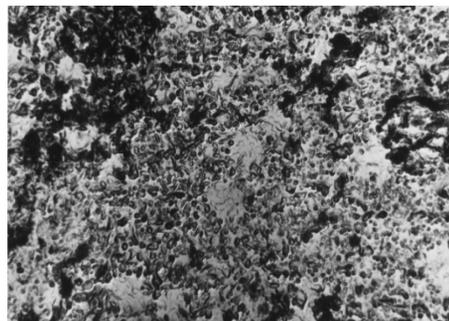
Fig. 5. Microstructure of steel involving an electric furnace desulfurized and argon refining (EA) and hardened and tempered at 600°C. Sphroidit – globular cementite in ferrite matrix. Mag. 2000x

Examples of typical non-metallic inclusions in steel produced in every analyzed process are presented in Figures 6-8. Al_2O_3 inclusions in the shape of irregular polyhedrons, small spherical MgO inclusions (Fig. 6), spherical MgO inclusions and Cr_2O_3 parallelepiped inclusions (Fig. 7), $SiO_2 \cdot CaO \cdot MnO$ multiphase inclusions (Fig. 8).
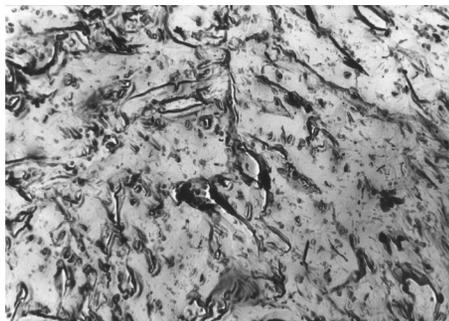
Fig. 6. Al_2O_3 inclusions in the shape of irregular polyhedrons, small spherical MgO inclusions. Process (E). Mag. 10 000x
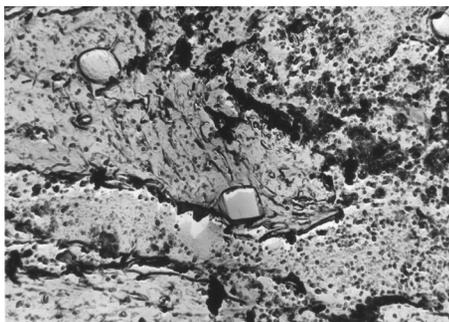
Fig. 7. Spherical MgO inclusions; Cr_2O_3 parallelepiped inclusions. Process (EA). Mag. 10 000x

Fig. 8. SiO$_2$·CaO·MnO multiphase inclusions deformed during processing. Process (KP). Mag. 10 000x

The curves illustrating the distribution of variously sized impurities are determined mainly by the relative volume of particles not exceeding 15 μm, in particular submicroscopic inclusions. Inclusions larger than 25 μm have an indirect influence (Fig. 9). It should be noted that the presence of large and brittle inclusions in the microstructure of steel subjected to fatigue loading can lower the material's fatigue strength.
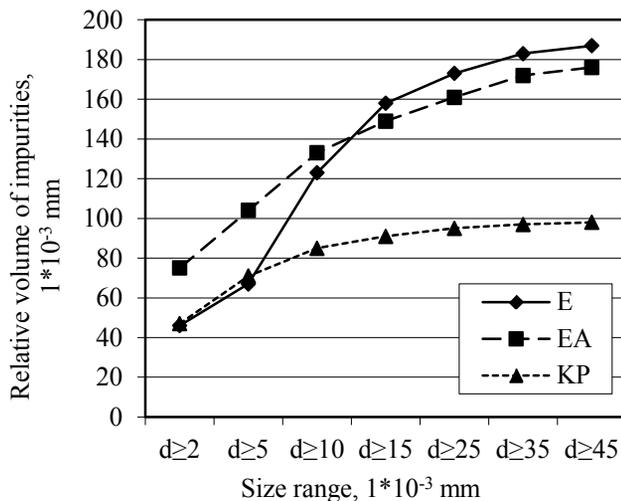
Fig. 9. Distribution of the relative volume of impurities, subject to size range

The average relative volume of non-metallic inclusions with a submicroscopic size of d<2 μm was highest in argon-refined steel melted in an electric furnace (EA). The investigated parameter was 29% lower in desulphurized steel melted in an electric furnace (E) and 36% lower in vacuum-degassed steel melted in a converter (KP). In the remaining size ranges, the highest relative volume of impurities was noted in desulphurized steel melted in an electric furnace (E), followed by argon-refined steel melted in an electric furnace (EA) and vacuum-degassed steel melted in a converter (KP).

Regression equations describing the correlations between the number of sample-damaging cycles and variable, fatigue-inducing loads are shown in Figures 10-12. At every tempering temperature, the highest number of cycles was reported for steel

tempered at low temperatures and the lowest number of cycles – for steel tempered at high temperatures.
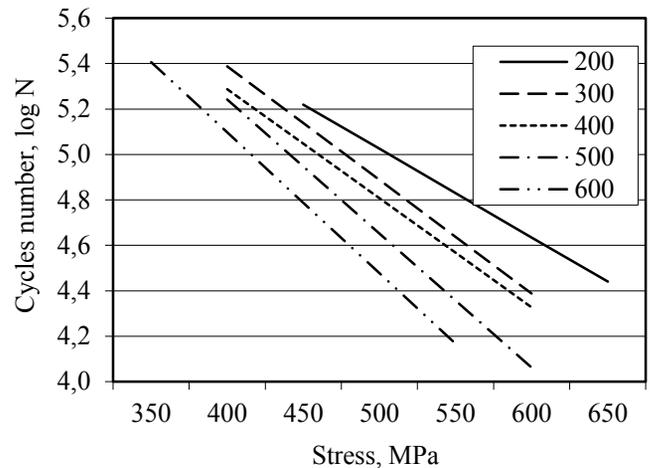
Fig. 10. Fatigue strength – regression lines for desulfurized steel melted in an electric furnace (E), hardened and tempered at 200, 300, 400, 500 and 600ºC
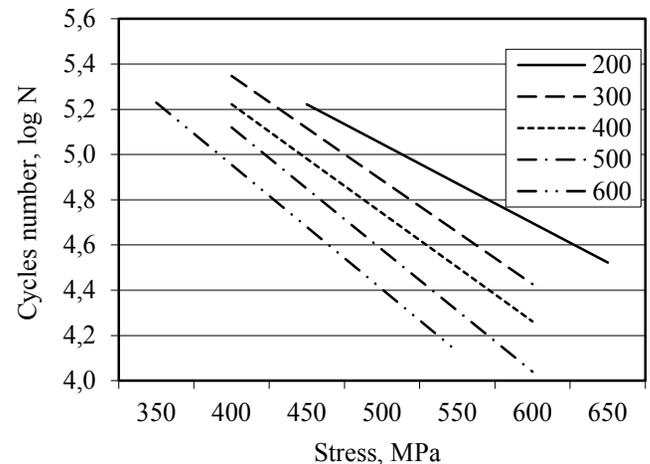
Fig. 11. Fatigue strength – regression lines for argon-refined steel melted in an electric furnace (EA), hardened and tempered at 200, 300, 400, 500 and 600ºC

For vacuum-degassed steel melted in a converter, the curves show similar values of logN in the load range of 400-450 MPa, excluding a tempering temperature of 200 and 600ºC. The reported range of logN values was significantly smaller in comparison with the remaining production methods shown in Figures 10 and 11.

The values of correlation coefficients and parameters used to verify statistical hypotheses indicate that the regression equations reliably represent the correlations between the tested properties and that errors were not made in the process of approximating the relationship with a linear function.

The location of the regression line suggests that steel durability increases with hardness and that trait variability is determined largely by out-of-furnace treatment. Steel melted in electric furnaces, (E) and (EA), was characterized by similar ranges of variation in durability and hardness, whereas the parameters of vacuum-degassed converter steel (KP) were characterized by a much lower scatter of results. A graphic distribution of fatigue strength parameters is shown in Figure 13.
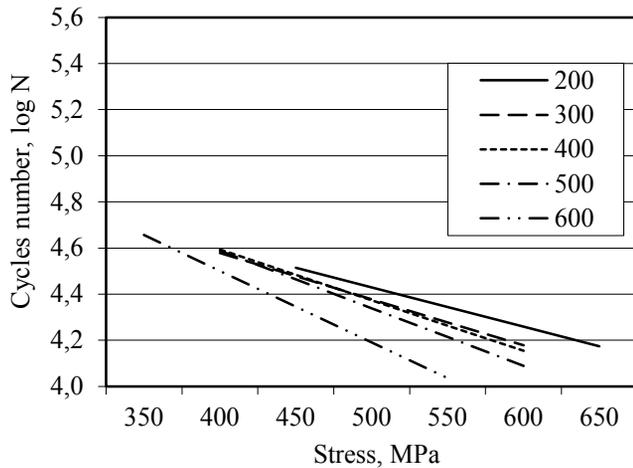
Fig. 12. Fatigue strength – regression lines for steel melted in a converter (KP), hardened and tempered at 200, 300, 400, 500 and 600°C
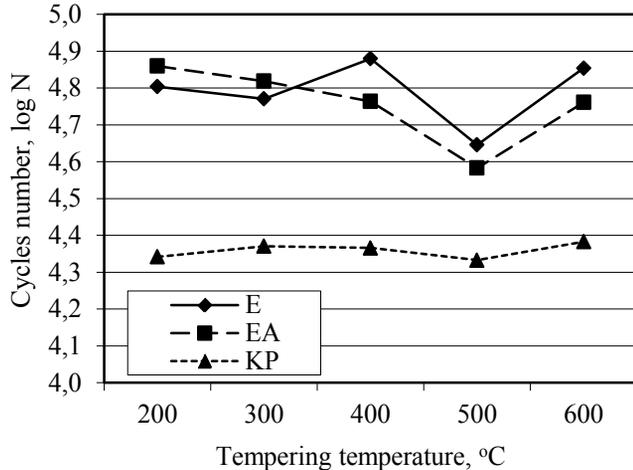
Fig. 13. Average number of sample-damaging cycles, traits in groups

No variations in fatigue strength parameters were observed between desulphurized steel (E) and argon-refined steel (EA). A significant drop in the number of sample-damaging cycles was reported in vacuum-degassed steel melted in a converter (KP). Converter steel (KP) was characterized by lower fatigue strength than the remaining steel types. At tempering temperature of 200 and 300°C, the highest fatigue strength values were noted in (EA) steel, whereas at higher tempering temperatures, desulphurized steel (E) was marked by the greatest fatigue strength. It can be

assumed that at low tempering temperatures, large non-metallic inclusions (Fig. 9) further contribute to the brittleness of tempered martensite.

The average endurance limit values for various heat processing options are presented in Figure 14.
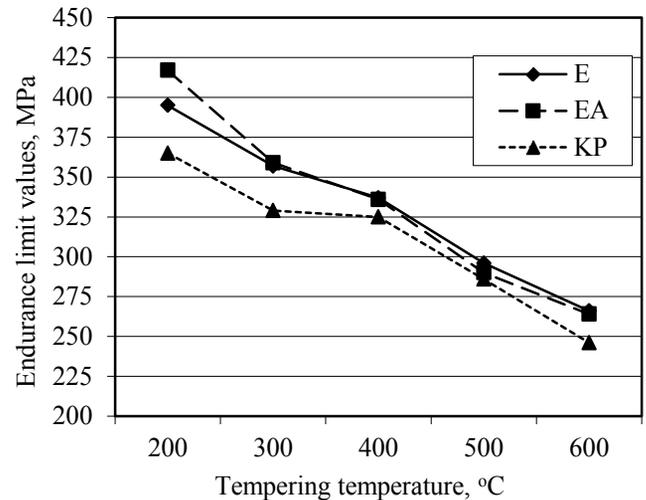
Fig. 14. Endurance limit values for various heat processing options

The values of the studied parameters decreased with an increase in tempering temperature. The parameters of desulphurized steel (E) and argon-rafined steel (EA) did not differ significantly (within the limits of error). Vacuum-degassed converter steel (KP) was characterized by the lowest endurance limit within the analyzed temperature range. Within the 300-600°C range, its endurance limit decreased by approximately 35%.

Fatigue strength coefficients are presented in Figure 15.
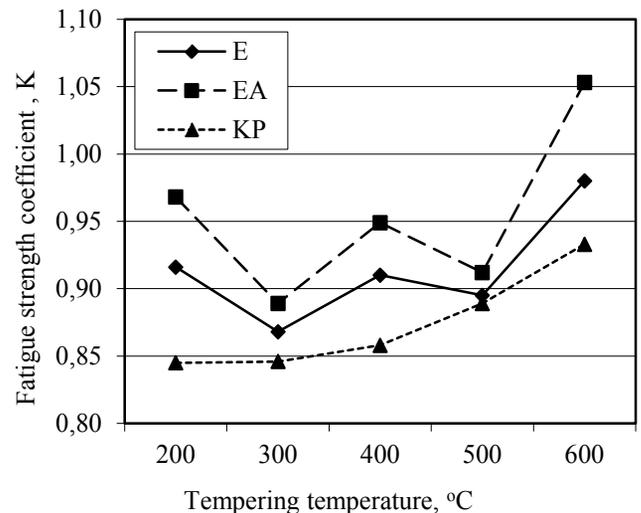
Fig. 15. Average values of the fatigue strength coefficient for different heat processing options

For the entire range of tempering temperatures, the highest fatigue strength was reported for argon-refined steel (EA), and the lowest – for vacuum-degassed converter steel (KP). In converter steel, changes in fatigue strength parameters approximated a linear function within the analyzed range of tempering temperatures. The value of the fatigue strength coefficient of steel melted in an electric furnace (E) was several percent higher in comparison with converter steel (KP), and it was characterized by higher variability. The highest fatigue strength coefficient was noted in argon-refined steel (EA) which was several percent higher than the coefficient for (E) steel.

4. Conclusions

The results of the presented experiment indicate that the production process of high-grade, low-alloy structural steel has a considerable effect on the structure of impurities and the fatigue strength of steel used in machines which operate under variable load.

The production process, in particular out-of-furnace treatment, determines the number and the structure of inclusions.

Vacuum-degassed converter steel (KP) contained the smallest number of impurities.

Vacuum degassing lowers the susceptibility of fatigue strength to the oscillation of stresses which cause decohesion.

A comparison of fatigue properties and the size of impurities suggests that submicroscopic inclusions in high-plasticity steel inhibits dislocation motion. Inclusions absorb energy which contributes to the formation of discontinuities and slows down decohesion.

References

[1] Borowiecki B., Borowiecka O., Szkodzińka E. (2011). Casting defects analysis by the Pareto method. *Archives of Foundry Engineering*. *11* (Special Issue 3), 33-36.

[2] Gajewski M., Kasińska J. (2009). Rare earth metals influence on morphology of non-metallic inclusions and mechanism of GP240GH and G17CrMo5-5cast steel cracking. *Archives of Foundry Engineering*. *9*(4) 45-52.

[3] Lipiński T., Wach A. (2010). The effect of the production process of medium-carbon steel on fatigue strength. *Archives of Foundry Engineering*. *10*(2), 79-82.

[4] Senberger J., Zadera A., Cech J. (2011). Checking the metallurgy with the aid of inclusion analysis. *Archives of Foundry Engineering*. *11*(1) 118-122.

[5] Lipiński T., Wach A. (2009). The effect of out-of-furnace treatment on the properties of high-grade medium-caborn structural steel. *Archives of Foundry Engineering*. *10*, 93-96.

[6] Wypartowicz J., Podorska D. (2005). The influence of non - metallic inclusions in steel with progressive solidification. *Hutnik - Wiadomości Hutnicze*, 1 (in Polish).

[7] Lipiński T., Wach A. (2010). The Share of Non-Metallic Inclusions in High-Grade Steel for Machine Parts. *Archives of Foundry Engineering*. *10*(SI 4), 45-48.

[8] Kalandyk B. (2006). The Influence Of The Deoxidation And Modification On The Morphology Of Non-Metallic Inclusion In The Carbon Cast Steels. *Archives Of Foundry*. *6, Nᵒ 18* (1/2), 419-424.

[9] Roiko A., Hänninen H., Vuorikari H. (2012). Anisotropic distribution of non-metallic inclusions in a forged steel roll and its influence on fatigue limit. *International Journal of Fatigue*. *41*, 158–167.

[10] Miner M.A. (1945). Cumulative damage in fatigue. *Trans. ASM. 65*, 159-165.

[11] Kocańda S. (1985). Zmęczeniowe pękanie metali. Warsaw: WNT (in Polish).

[12] Pyttel B., Schwerdt D., Berger C. (2011). Very high cycle fatigue – Is there a fatigue limit? *International Journal of Fatigue. 33*, 49-58.

[13] Lis T. (2002). Modification of non-metallic dispersion phase in steel. *Metallurgy and Foundry Engineering. 1/28,* 29-45.

[14] Murakami Y. (2002). Metal fatigue, Effects of small defects and nonmetallic inclusions, Oxford, Elsevier 57–115.

[15] Yang Z.G., Li S.X., Li Y.D., Liu Y.B., Hui W.J., Weng Y.Q. (2010). Relationship among fatigue life, inclusion size and hydrogen concentration for high-strength steel in the VHCF regime. *Materials Science and Engineering A. 527*, 559-564.

[16] Ekengren J., Bergström J. (2012). Extreme value distributions of inclusions in six steels. *Extremes. 15*, 257-265.

[17] Saberifar S., Mashreghi A.R., Mosalaeepur M., Ghasemi S.S. (2012). The interaction between non-metallic inclusions and surface roughness in fatigue failure and their influence on fatigue strength. *Materials and Design. 35,* 720-724.

[18] Costa N., Silva F.S. (2011). On a new temperature factor to predict the fatigue limit at different temperatures. *International Journal of Fatigue. 33,* 624-631.

[19] Kailash C. Jajam, Hareesh V. Tippur (2012). Role of inclusion stiffness and interfacial strength on dynamic matrix crack growth: An experimental study. *International Journal of Solids and Structures. 49,* 1127-1146.

[20] Lipiński T., Wach A. (2009). Non-metalic inclusions structure dimension in high quality steel with medium caborn contents. *Archives of Foundry Engineering.* 9, 75-78.